1 General Reply

Thank you very much for your second review of our article. As with the previous review, your detailed comments helped us to write a better, more comprehensive paper.

We have considered all your comments and included many of your suggested changes in the revised manuscript.

Find below your original comments (in italics), the specific responses, and the changes made to the manuscript (in blue).

Sebastian Rhode, on behalf of all authors

1.1 General comment

I would like to thank the authors of the manuscript "A mountain ridge model for quantifying oblique mountain wave propagation and distribution" for their thorough review, explanations, and friendly response. I think the manuscript has significantly improved but still requires some minor changes. Besides some minor comments, I figured out that the used blocking diagrams are violating the authors' assumptions and need replacement. A possible strategy is suggested below in the individual comments. With these suggested changes added to the manuscript, I will happily recommend it for publication. Please note that all line numbers refer to the manuscript version 2.

Thank you again for your thorough review. We have addressed your specific comments below. In addition, we want to thank you for your constructive suggestion of a different kind of blocking diagram. We are happy to include this in our article as another analysis tool. The original blocking diagrams, as done in Taylor et al. [1993], are still kept in the manuscript to grant an investigation of the propagation conditions for non-orographic GWs.

The manuscript has received another overhaul, thanks to your suggestions.

1.2 Specific comments

1. *Response #14 and #15 are convincingly explained in the response but not reflected by a hint in the text. It would be nice if the authors could add corresponding comments.*

   We assume this comment refers to #13 and #15 since we added a new section in response to #14.

   Regarding the response to #13, we added another paragraph clarifying the difference in scale separation for the HIRDLS retrieval and the ray-tracing background generation: "Note that the scale-separation methodology of the ERA5 data used for background removal differs from the generation of the ray-tracing backgrounds. Since we are interested in the GW content of the measurements, we need to carefully remove the larger-scale dynamics, such as Rossby waves, from the background field. In the lower stratosphere, these can reach zonal wavenumbers as high as 6, but considerably higher in the troposphere, which is why the filter is designed with a linear decrease of cutoff wavenumber with altitude. The ray-tracing simulations are not as sensitive to small remnants of smaller-scale dynamics, and, therefore, the scale separation described in Strube et al. [2020] is used there."

   Regarding the response to #15, we added the following sentences to the manuscript: "The use of overlapping bins introduces spatially dependent auto-correlations to some extent, which leads to smearing out of the global distribution. The advantage is, however, an increase in statistics for each bin."

2. *L6 - location -¿ locations*

   This mistake is corrected in the revised version.

3. *L144 - the projection is still unclear - projecting onto an equidistant grid from 10° slices is not clear*

   We resample the longitude grid onto a 1' latitude equivalent at the center of the topography slice. In this way, the grid is equidistant at the center. The longitude spacing, however, is still increasing (decreasing) equator-ward (pole-ward).

The text in the manuscript was changed to:

"The longitudes of the topography slice are resampled onto a 1' latitude, or about 1.85 km, equivalent grid (at the meridional center), such that the resulting grid is equidistant in the center. The grid distance is, however, still increasing equator-ward (decreasing pole-ward). This resampling mitigates possible errors in the scale separation and fitting of ridge widths and lengths due to differently scaled dimensions at high latitudes."

4. *38 - the authors explain their usage of the chirp rate, maybe mentioning in the text a little clearer would be great*

   We edited the text to describe the effect of the approximation and which particular term is approximated by the chirp rate c_m in a better way.

   The corresponding section has been reworked to: "The last term accounts for a linear approximation of the change in vertical wavelength along the vertical with chirp rate $c_\mathrm{m} = \frac{\Delta_\mathrm{m}}{\Delta_z}$ and $m(z) \approx m(z_0) + c_\mathrm{m} d_z + \mathcal{O}(d_z^2)$. The chirp rate is calculated as the finite difference derivative of m for the closest time steps around target altitude z. The linear approximation of the dependence of the vertical wavelength on altitude increases the reconstruction performance significantly where it changes rapidly, e.g. below critical layers [e.g. Nappo, 2012]. In testing, we found that considering only the leading order, i.e., $m(z) \approx m(z_0)$, leads to inconsistent phase transitions between wave packets excited by the same mountain ridge at different times."

5. *Sec. 3.2 - It would be great to remind the reader of the lower boundary condition in the description of the raytracer.*

   We added a brief recapitulation of the lower boundary condition as required for GROGRAT at the beginning of section 3.2: "In this framework, the lower boundary condition for each individual GW is given by the location (longitude, latitude, and altitude) and launch time, the horizontal wave vector (k, l), the initial amplitude, and the ground-based frequency."

6. *L239 - The amplitude correction was added to the appendix by the authors, it would be great if they would also mention some results and reason why they do not go forward with the calculated correction in the main body. In particular, the nice results raise the question of why this has not been taken into account throughout the whole study.*

   A few sentences to the general findings were added below the reference to App. D: "In our specific investigation, this correction leads to unchanged GW amplitudes (horizontally) close to the sources and enhanced amplitudes for GWs propagating far from the sources. Since horizontal deformation of the wave packet is caused by refraction, turning, and changing backgrounds, laterally far propagating GWs are especially prone to this effect."

   Our main reason for not including the correction in this study is to be consistent with previous studies focusing on ray-tracing in GROGRAT. The currently-used amplitude calculation has been used in a number of studies with validation to observations [Preusse et al., 2009, Krisch et al., 2017, Krasauskas et al., 2023]. Compared to this the approximated ray-tube method is less well validated and deserves a dedicated study to be properly introduced and tested. We here give first results in App. D to demonstrate the size of the effect.

   The following reasoning was added to the text: "Although the results in App. D are reasonable, for consistency with previous studies we are not taking the correction into account here, and all following simulations of this study are performed with the standard GROGRAT amplitude calculation.

   Although the results in App. D are reasonable for consistency with previous studies, we are not taking the correction into account here, and all following simulations of this study are performed with the standard GROGRAT amplitude calculation. The currently-used method of ignoring the last term in Eq. 6 has been used in a number of studies with validation to observations [Preusse et al., 2009, Krisch et al., 2017, Krasauskas et al., 2023]. Compared to this, the approximated ray-tube method is less well-validated and deserves a dedicated study to be properly introduced and tested. Therefore, we give only first results in App. D for a demonstration of the size of the effect."

7. *L303f - The authors provide a nice justification for the 3x3 choice in the response which is, however, not reflected in the manuscript. I would suggest adding a sentence that the expected errors given the subsampling are of the order of a couple of percents as quantified in the response.*

   That is a good point. The following sentence was added to the manuscript after the description of the calculation: "We estimated the error of this approximation to be below $\sim 5\%$ for randomly oriented GWs of 100 km horizontal wavelength and decreasing for longer GWs."

8. *Sec. 4.1 - The new figures for the other regions are indeed a nice addition to the manuscript. It would be nice if the analysis in Appendix C was referenced in Sec. 4.1.*

   Indeed, there was little advertising for this appendix. This was fixed by including of the following sentence:

   "More detail on the reconstruction of the southern Andes topography for different scales and a similar analysis for the Himalaya and South Africa region, considered later on in this study, is given in App. C."

9. *L370ff - "The IFS data shows high activity of all scales above the oceans as well at this height, which indicates either wave sources other than orography (e.g. convection, jet fronts, and geostrophic (or spontaneous) adjustment, where an out-of-balance jet radiates excessive energy as inertia-gravity waves (e.g. Fritts and Alexander, 2003; Williams et al., 2003; de la Camara and Lott, 2015)) or completely different tropospheric processes, that our scale separation anomalously picks up. However, the MWM also shows a large-scale pattern to the east of the continent, which might indicate that orographic GWs of large-scale (and therefore higher horizontal group velocity) might also add to the patterns seen in the IFS."*

   - Here the line of argument needs to be disentangled. The point of comparison to the IFS is the validation of the MWM. However, the authors rather interpret the IFS and suggest shortcomings to the scale separation in postprocessing the IFS data instead. This interpretation would be premature for a non-validated dataset. I suggest the authors reframe the argument into the interpretation of the differences in terms of the MWM rather than evaluating the IFS based on the MWM.

   This section was framed the wrong way around and was therefore changed corresponding to your comment to: "Nevertheless, the MWM data exhibits a large-scale pattern to the east of the continent above the Pacific Ocean, indicating that MWs of comparatively large scales (and thus high horizontal group velocity) are strongly propagating below the tropopause. And indeed, we see similar structures in the IFS model data. Note, however, that the IFS models GWs of all sources, and therefore, the seen features could be (partly) due to convection, jet fronts, and geostrophic (or spontaneous) adjustment (where an out-of-balance jet radiates excessive energy as inertia-gravity waves [e.g. Fritts and Alexander, 2003, Williams et al., 2003, de la Camara and Lott, 2015]) or even other tropospheric processes, that are not filtered out well in our scale separation."

10. *LL450-454 - The authors describe the patterns found in the HIRDLS dataset, but do not mention the latter. I suggest the authors clarify which dataset the described observation is associated with.*

    We tried to use the phrasing "observation" only for the HIRDLS measurements, but indeed this is not very clear in general. Thus the text was changed according to your comment:

    "The strongest pattern in the HIRDLS observations is found above..."

11. *L496, Fig. 6 - blocking diagrams Surprisingly I have not seen some inconsistencies concerning the blocking diagrams in the first round of reviews. I think, however, that the blocking diagrams are not applicable in the here presented form. First of all, equation 12 is generally singular for mountain waves. Dividing by ω_{gb} is only permissive where it is non-zero and additionally contradicts the interpretation of the blocking diagram where it is assumed to be approximately zero (c.f. lines 506 and 515). Moreover, the rotation was neglected by assuming a minimum intrinsic frequency equal to zero. Finally, I am under the impression*

that the authors misinterpret the figures of Taylor et al. 1993. Their blocking diagrams are plotted in terms of the background wind (U, V) (admittedly their axes lack labels) rather than phase speeds. Moreover, description in terms of ground base phase speeds (as done here) for orographic waves would be trivial as they are always approximately zero. The present interpretation of Fig. 9 thus directly violates the quasi-stationary nature of mountain waves. I thus suggest the following procedure instead:# Rewriting equation 11 - under the assumption of an approximately zero ground-based frequency and a quasi-steady wind - one may find that

$$f < \omega_{intr} = -|\vec{U}||\vec{k}_{hor}|\cos(\alpha), \tag{1}$$

where α is the angle between the horizontal wind and wave vectors. One may thus find all regions where the above relation is violated (corresponding to the critical filtering) as a function of the zonal and meridional wavenumbers within the target area and altitude range. The probability then depends on the observed wind directions (relative to the wave vector) as well as the wind amplitude. Visualizations similar to Fig. 9 but depending on the wavenumbers (k, l) instead would then give a probability of critical layer filtering given the initial wavenumber pair.

Yes, it is correct that these blocking diagrams give only a hint at the filtering of mountain waves (with $\omega_{\mathrm{gb}} \approx 0$). However, they give a good impression of regions within the phase speed that are critical level filtered for GWs of other origin (or even MWs far from their source, where the transient background field has shifted gb away from 0).

The diagrams in Taylor et al. [1993], however, do show phase speed spectrum and the restricted regions due to the external wind. Although the restricted areas depend on the background wind speeds, the diagram axis are given as the phase speed in zonal and meridional direction. Indeed the missing description and axes labeling are misleading, the corresponding text in Taylor et al. [1993], however, clarifies that phase speeds are considered.

Our main aim in using the blocking diagrams is to look at the restrictions for non-orographic waves and thereby explain the different change in GWMF in the HIRDLS observations and the MWM predictions, since HIRDLS observes much more than we model within the MWM. In the revised version, we tried to make the focus on the non-orographic GWs more clear.

Indeed, the Coriolis frequency has been left out for this consideration similar to the work of Taylor et al. [1993]. The framework of blocking diagrams gives nevertheless a good first look at the restrictions in phase speed space. To clarify that f is neglected, we added the following sentence to the manuscript: "In addition, the Coriolis parameter is neglected within this consideration, which would restrict the intrinsic frequency even more ($|f| < \omega_{\mathrm{intr}}$) and hence leads to a stronger restriction of phase speeds."

Your suggestion of a different type of blocking diagram is very good and we like to add this to our analysis. Since the article is already quite long, this has been shifted to the Appendix. The following paragraph was added to the main text: "Since the here considered blocking diagrams are not directly applicable to MWs close to their sources, we additionally show alternative blocking diagrams for MWs with $\omega_{\mathrm{gb}} \approx 0$ in App. E. Figure E1a and c show that due to the wind profile, the (horizontal) phase space in the Himalaya region is less restricted and, therefore, might exhibit more (diverse) MW activity in the stratosphere. The Mongolian Plateau, on the other hand, shows a much more restricted initial phase space. This underlines that the strong northward shift of the maximum in the HIRDLS observations compared to the MWM could stem partly from non-orographic GWs measured above the northern part as well as MWs refracting to vertical wavelengths that the observation data does not pick up."

The corresponding Appendix E reads as follows:

Appendix E: Mountain Wave blocking diagrams

Since the blocking diagrams described in Taylor et al. [1993] are not directly applicable to orographic GWs close to their source where $\omega_{\mathrm{gb}} \approx 0$, we show a different type of blocking diagram in this section. The considerations are based on the relation of wave vector to intrinsic frequency and the lower limit for the frequency of GWs:

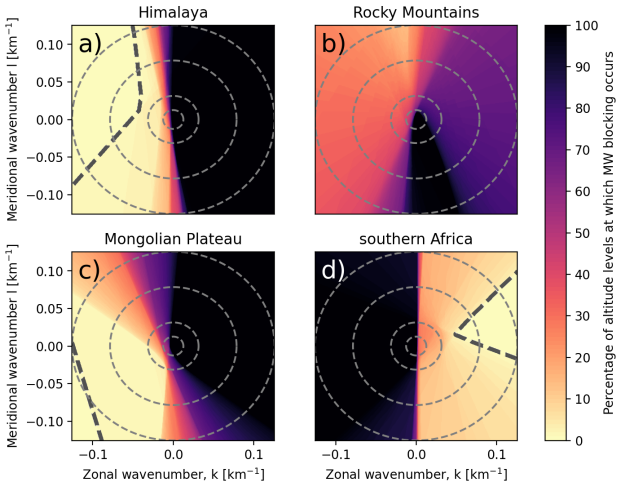

Figure E1: Mountain wave blocking diagrams similar to the ones given in Fig. 9 but more applicable for MWs with $\omega_{\mathrm{gb}} \approx 0$. In this case, the critical level filtering is based on the wind profile and Eq. 3. The percentage of altitudes from the surface to 25 km at which an MW of given horizontal wavenumbers is blocked is given in color shading. The dashed line separates the region of (horizontal) phase space that does encounter no critical level at any level (radially outwards w.r.t. the dashed line). Circular gird lines show horizontal wavelengths of 500 km, 200 km, 80 km, and 50 km (from the center outwards). Note that this diagram does not consider refraction, which could lead to MWs maneuvering around critical levels in phase space on their propagation path.

$$\omega_{\mathrm{intr}} = -kU - lV, \tag{2}$$

$$\omega_{\mathrm{intr}} \overset{!}{\geq} |f|. \tag{3}$$

Here f is the Coriolis parameter, k and l are the zonal and meridional wavenumbers, and U and V are the zonal and meridional background wind speeds. Combining both equations allows an estimation where the intrinsic frequency drops below the Coriolis frequency for a given wind speed and direction, which directly corresponds to a critical level for MWs and therefore restricts vertical propagation.

Figure E1 shows the restricted (horizontal) phase space for the same regions and wind profiles as Fig. 9a – d. Panels a and c show the Himalaya and Mongolian Plateau region, respectively, where basically the opposite of the more general blocking diagrams can be seen. While Fig. 9 shows that the Himalaya region has the more restricted phase speed space for non-orographic GWs, for GWs of orographic origin, the Himalaya region shows a more favorable phase space. Only half the phase space is strongly restricted here, while about two-thirds are restricted above the Mongolian Plateau. This strengthens our finding that the northward shift seen in the HIRDLS observations is due to stronger non-orographic GWs in the northern region and MWs refracting to large vertical wavelengths in the southern region.

The Rocky Mountain region in Fig. E1b is highly restricted for mountain waves, as is expected due to the wind reversal, and therefore almost no MWs will reach up to 25 km altitude. Although there is a hint at a wind reversal in the vertical wind profile of the southern Africa region, this is not confirmed by Fig. E1d, where a large part of the GW spectrum is blocked, but by far not the full phase space as in Fig. E1b. The weak surface level winds (c.f Fig. 9f) are, however, very unfavorable conditions to launch and propagate MWs to the stratosphere in the first place.

12. *L519 - blocking -> critical layer filtering*

This was changed accordingly in the revised version.

13. *L726 - "Using the ray-tracer GROGRAT [...]" -¿ Using a modified version of the ray-tracer GROGRAT...*

    This was changed accordingly in the revised version.

References

A. de la Camara and F. Lott. A parameterization of gravity waves emitted by fronts and jets. *GEOPHYSICAL RESEARCH LETTERS*, 42(6):2071–2078, MAR 28 2015. ISSN 0094-8276. doi: 10.1002/2015GL063298.

D. Fritts and M. Alexander. Gravity wave dynamics and effects in the middle atmosphere. *Rev. Geophys.*, 41(1), APR 16 2003. ISSN 8755-1209. doi: 10.1029/2001RG000106.

L. Krasauskas, B. Kaifler, S. Rhode, J. Ungermann, W. Woiwode, and P. Preusse. Oblique propagation and refraction of gravity waves over the Andes observed by GLORIA and ALIMA during the SouthTRAC campaign. *J. Geophys. Res. Atmos.*, page e2022JD037798, 2023. doi: 10.1029/2022JD037798.

I. Krisch, P. Preusse, J. Ungermann, A. Dörnbrack, S. D. Eckermann, M. Ern, F. Friedl-Vallon, M. Kaufmann, H. Oelhaf, M. Rapp, C. Strube, and M. Riese. First tomographic observations of gravity waves by the infrared limb imager GLORIA. *Atmos. Chem. Phys.*, 17(24):14937–14953, 2017. doi: 10.5194/acp-17-14937-2017.

C. J. Nappo. *An Introduction to Atmospheric Gravity Waves.* Academic Press, second edition, 2012. ISBN 978-0-12-385223-6.

P. Preusse, S. D. Eckermann, M. Ern, J. Oberheide, R. H. Picard, R. G. Roble, M. Riese, J. M. Russell III, and M. G. Mlynczak. Global ray tracing simulations of the SABER gravity wave climatology. *J. Geophys. Res. Atmos.*, 114, 2009. doi: 10.1029/2008JD011214.

C. Strube, M. Ern, P. Preusse, and M. Riese. Removing spurious inertial instability signals from gravity wave temperature perturbations using spectral filtering methods. *Atmos. Meas. Tech.*, 13(9):4927–4945, 2020. doi: 10.5194/amt-13-4927-2020. URL `https://amt.copernicus.org/articles/13/4927/2020/`.

M. J. Taylor, E. H. Ryan, T. F. Tuan, and R. Edwards. Evidence of preferential directions for gravity wave propagation due to wind filtering in the middle atmosphere. *J. Geophys. Res.*, 98: 6047–6057, 1993. doi: 10.1029/92JA02604.

P. D. Williams, P. L. Read, and T. W. N. Haine. Spontaneous generation and impact of inertia-gravity waves in a stratified, two-layer shear flow. *Geophysical Research Letters*, 30(24), 2003. doi: https://doi.org/10.1029/2003GL018498. URL `https://agupubs.onlinelibrary.wiley.com/doi/abs/10.1029/2003GL018498`.